Acta Cryst E CRYSTALLOGRAPHIC COMMUNICATIONS

ISSN 2056-9890

Crystal structure and Hirshfeld surface analysis of the coordination compound diaqua[5,10,15,20-tetrakis(4-chlorophenyl)porphyrinato-κ^4N]-magnesium(II)

Mona A. Alamri*

Department of Chemistry, College of Science, Qassim University, Buraidah 52571, Saudi Arabia. *Correspondence e-mail: M.alamri@qu.edu.sa

Received 5 January 2026
Accepted 27 January 2026

Edited by B. Therrien, University of Neuchâtel, Switzerland

Keywords: crystal structure; magnesium(II) porphyrin; diaqua complex; intermolecular interactions; Hirshfeld analysis.

CCDC reference: 2526366

Supporting information: this article has supporting information at journals.iucr.org/e

During the synthesis of the (oxalato)[5,10,15,20-tetrakis(4-chlorophenyl)-porphyrinato]magnesium(II) ([Mg(TClPP)(ox)]) complex [TClPP = 5,10,15,20-tetrakis(4-chlorophenyl)porphyrinate and ox = oxalate], the title compound, $[Mg(C_{44}H_{24}ClMgN_4O_2)(H_2O)_2]$ ($[Mg(TClPP)(H_2O)_2]$), was obtained as a by-product. The diaqua–Mg^{II} porphyrin complex crystallizes in the $I4/m$ space group. In the asymmetric unit, except for two carbon atoms of the phenyl ring, all atoms lie on special positions. In the crystal, the $[Mg(TClPP)(H_2O)_2]$ molecules form layers parallel to the a axis. The crystal packing features C—H$\cdots\pi$ interactions involving the pyrrole rings and non-conventional O—H$\cdots$Cl hydrogen bonds between the oxygen atom of the water axial ligands and the chloride of neighboring phenyl groups. Hirshfeld surface analysis indicates that intermolecular contacts are dominated by H$\cdots$H (50.2%), followed by H$\cdots$Cl (21.6%) and H$\cdots$C (21.2%) interactions, then by less chemically meaningful C$\cdots$Cl (6.0%) contacts.

1. Chemical context

Magnesium, the eighth most abundant element in the Earth's crust and an essential nutrient for all living organisms, plays a central role in biological processes, most notably as the coordinating metal ion in chlorophyll, the photosynthetic pigment that sustains life on Earth (Barker & Pilbeam, 2015). The coordination chemistry of magnesium(II), particularly within porphyrin frameworks, has thus attracted sustained scientific interest due to its fundamental relevance to photosynthesis and its potential in bioinspired technologies (Borah & Bhuyan, 2017).

The foundation of magnesium(II) metalloporphyrin chemistry was laid in the early to mid-20th century. One of the pioneering contributions came from Hans Fischer, whose extensive work on porphyrin synthesis and metal insertion in the 1930s and 1940s provided the first systematic routes to metalloporphyrins, although Mg^{II} complexes were often challenging to isolate due to their lability in protic media (Fischer *et al.*, 1937). Later, the structural elucidation of chlorophyll by Robert Burns Woodward and colleagues in the 1960s, culminating in the total synthesis of chlorophyll *a* offered profound insight into the unique coordination environment of Mg^{II} in natural porphyrinoids, notably the presence of a fifth and sixth axial ligands and the susceptibility of the Mg—N bonds to hydrolysis (Woodward *et al.*, 1960).

Unlike transition metals that form robust metalloporphyrins, Mg^{II} porphyrins are diamagnetic, d^0 complexes with labile axial coordination sites, which imparts distinctive

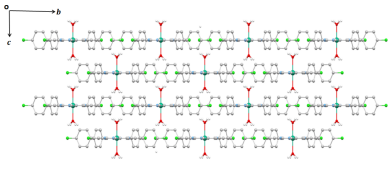

photophysical properties, but also presents synthetic challenges. Nevertheless, these attributes make Mg^{II} porphyrins particularly attractive for applications that require efficient light harvesting, energy transfer, and reversible ligand binding, all hallmarks of natural photosynthetic systems.

In recent years, synthetic Mg^{II} porphyrins have found utility beyond biology. They serve as key components in artificial photosynthetic devices, where they act as light absorbers and electron donors in photoinduced charge-separation systems (Gust *et al.*, 2001). For instance, several reported investigations have engineered tailored Mg porphyrins for integration into molecular triads and tetrads that mimic the primary events of photosynthesis, achieving long-lived charge-separated states relevant to solar energy conversion (Borah *et al.*, 2017). Additionally, Mg^{II} porphyrins have been employed as sensors (Gutiérrez *et al.*, 2014). More recently, they have been explored in photocatalysts for the transformation of CO_2 to cyclic carbonates and oxazolidinones (Meher *et al.*, 2024).

Accordingly, the controlled synthesis, stabilization, and functionalization of Mg^{II} porphyrins remain active areas of research, driven by both fundamental curiosity and the pursuit of sustainable technologies inspired by nature's design. Herein we report the synthesis, the single crystal X-ray molecular structure and the Hirshfeld surfaces analysis of the title diaqua[{5,10,15,20-tetrakis(4-chlorophenyl)}porphyrinato-κ^4N]-magnesium(II) coordination compound.

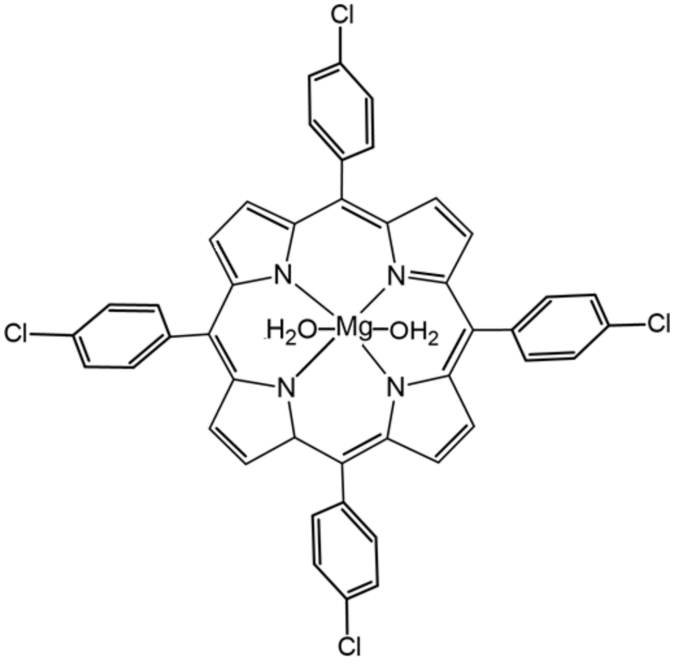

2. Structural commentary

The title compound crystallizes in the tetragonal space group *I4/m* (Fig. 1). The asymmetric unit comprises one quarter of the $[Mg(TClPP)(H_2O)_2]$ molecule leading to the formula $[Mg(C_{44}H_{24}ClMgN_4O_2)(H_2O)_2]$. The central Mg^{II} ion is coordinated to nitrogen atoms of the porphyrin core, and to oxygen atoms of the water molecules, thus showing an octahedral geometry.

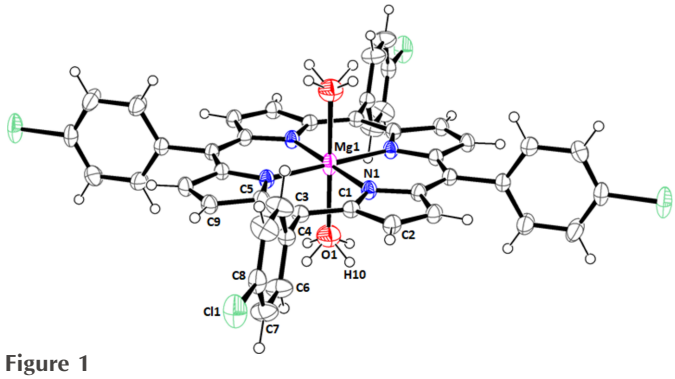

Figure 1
$[Mg(TClPP)(H_2O)_2]$ showing the atom labelling scheme. Displacement ellipsoids are drawn at the 40% probability level. All possible positions of the disordered H atoms of the water molecules are shown.

The $Mg—O(H_2O)$ distance of the $[Mg(TClPP)(H_2O)_2]$ complex is 2.248 (3) Å, which is in the normal range of bis-(aqua)–porphyrin complexes, *e.g.*, for the related $[Mg(TBrPP)(H_2O)_2]$ (TBrP = 5,10,15,20-tetrakis(4-bromophenyl)porphyrinate), the $Mg—O(H_2O)$ bond length is 2.221 (4) Å (Amiri *et al.*, 2015). Notably, the $[Mg(TBrPP)(H_2O)_2]$ related species is isotypic to our TClPP–magnesium-diaqua complex. In 2022, the structure of the $[Mg(TClPP)(pyz)][Mg(TClPP)(H_2O)_2]$ (pyz = pyrazine) complex was reported, for which $[Mg(TClPP)(pyz)]$ and $[Mg(TClPP)(H_2O)_2]$ are present in the same asymmetric unit (PELVUB; Singh *et al.*, 2022). For this $[Mg(TClPP)(H_2O)_2]$ coordination compound, the $Mg—O(H_2O)$ distance is 2.267 (5) Å, which is slightly longer than that of the title compound.

For the pentacoordinated monaqua–Mg^{II}–porphyrin complex [Mg(Porph)(H_2O)] (Porph = *meso*-arylporphyrinate), the $Mg—O(H_2O)$ bond length is shorter than those of the bisaqua magnesium(II) porphyrins such as the $[Mg(TPP)(H_2O)_2]$ complex, for which $Mg—O(H_2O)$ is 2.053 (5) Å (McKee & Rodley, 1988). The distance between the central Mg^{2+} ion and the N1 atom of the TClPP porphyrinate of $[Mg(TClPP)(H_2O)_2]$ ($Mg—N_p$) is 2.0646 (17) Å. For the related complexes $[Mg(TBrPP)(H_2O)_2]$ (Amiri *et al.*, 2015) and $[Mg(TClPP)(H_2O)_2]$ (Singh *et al.*, 2022), the average distances between the central Mg^{2+} ion and the four nitrogen atoms of the pyrrole rings of the porphyrin macrocycle (Mg—Np) are 2.069 and 2.082 Å, respectively. All these Mg—Np values are typical of magnesium(II) metalloporphyrins (Jabli *et al.*, 2022).

3. Supramolecular features

In the crystal, the $[Mg(TClPP)(H_2O)_2]$ complex molecules form layers parallel to the [100] direction (Fig. 2). As shown in Fig. 3, each oxygen atom of the two *trans* axial aqua ligands and the four symmetry-related atoms are involved in hydrogen bonds with the chlorine atom of a neighboring TClPP porphyrinate molecule with a distance of 3.691 (2) Å

Table 1
Hydrogen-bond geometry (Å, °).

*Cg*1 and *Cg*2 are the centroids of the N1,C1,C2,C9″,C5″ and C5,C9,C2′,C1′, N1′ rings, respectively. Symmetry codes: (′) $-y, -1+x, z$; (″) $1+y, -x, z$.

D—H···A	D—H	H···A	D···A	D—H···A
C7—H7···$Cg1^{i}$	0.95	2.75	3.608 (2)	150
C7—H7···$Cg2^{ii}$	0.95	2.75	3.608 (2)	150
O1—H10···$Cl1^{iii}$	1.01	2.92	3.691 (2)	128

Symmetry codes: (i) $y+\frac{1}{2}, -x+\frac{1}{2}, z+\frac{1}{2}$; (ii) $-x+\frac{1}{2}, -y-\frac{1}{2}, z+\frac{1}{2}$; (iii) $x+\frac{1}{2}, y-\frac{1}{2}, z+\frac{1}{2}$.

(Table 1). The crystal of the new Mg^{II}–diaqua–TClPP metalloporphyrin is further consolidated by C—H···π interactions between the carbon C7 of a phenyl of a TClPP porphyrinate and the centroid of the pyrrole rings of the porphyrin core with a C7···centroid distance of 3.608 (2) Å (Fig. 3., Table 1).

4. Database survey

A survey of the Cambridge Structural Database (CSD, version 6.00, update April 2025; Groom *et al.*, 2016) revealed 11 structures of aqua magnesium(II) porphyrin complexes. Among these porphyrinic coordination complexes, four are hexacoordinated diaqua complexes and seven are pentacoordinated monoaqua metalloporphyrins. The four reported diaqua–Mg^{II}–porphyrin complexes are: [Mg(T3,5-OMePP)-$(H_2O)_2$] (T3,5-OMePP = 5,10,15,20-tetrakis(3,5-dimethoxyphenyl)porphyrinate) (GOJGEV; Borah *et al.*, 2024), [Mg(TBPP)$(H_2O)_2$] (TPBPP = 5,10,15,20-tetrakis(4-(benzoyloxy)phenyl)porphyrinate) (CUCZAD; Amiri *et al.*, 2015), [Mg(TPP)$(H_2O)_2$](18-C-6) (TPP = 5,10,15,20-tetraphenylporphyrinate and 18-C-6 = 18-crown-6) (LERTAF; Ezzayani *et al.*, 2013) and [MgTClPP$(pyz)_2$][MgTClPP$(H_2O)_2$] (pyz = pyrazine) (PELVUB; Singh *et al.*, 2022). In this latter example, one half [Mg(TClPP)$(pyz)_2$] molecule and one half [Mg(TClPP)$(H_2O)_2$] molecule are both present in the asymmetric unit. The seven reported monoaqua Mg^{II} metalloporphyrins are: [Mg(TPP)(H_2O)]·2(C_6H_7N) (C_6H_7N = picoline) (DUJKUO; Ong *et al.*, 1986), [Mg(TPP)(H_2O)]·C_3H_6O (GEPBUY; McKee & Rodley, 1988), [Mg(T3,5-OMePP)-(H_2O)] (GUHXAL; Borah *et al.*, 2017), [Mg(TPBP)(H_2O)] (TPBP = 5,10,15,20-tetrakis(4-(benzoyloxy)phenyl)porphyrinate (HALDOR; Amiri *et al.*, 2022), [Mg(TMPP)(H_2O)] (TMPP = 5,10,15,20-tetrakis(4-methoxyphenyl)porphyrinate)

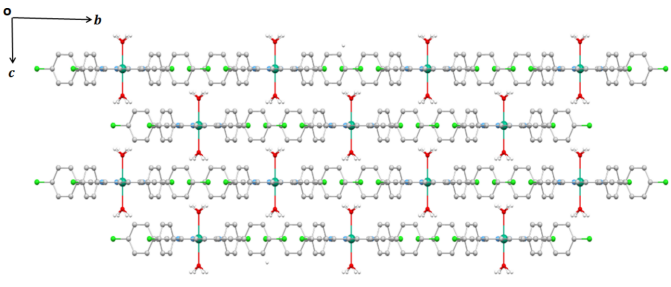

Figure 2
Packing viewed along the [100] direction showing the layers made by [Mg(TClPP)$(H_2O)_2$] complex molecules.

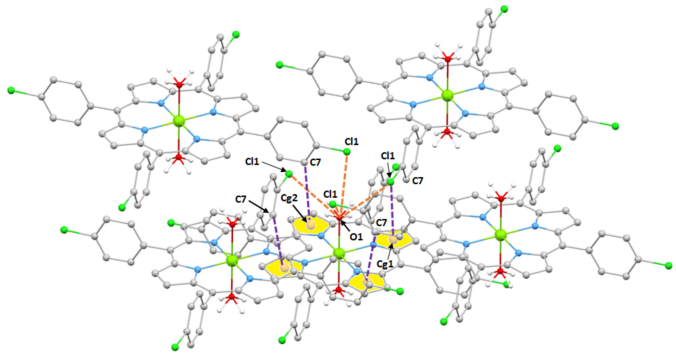

Figure 3
View showing the C—H···Cl and the C—H···*Cg* (*Cg* is the centroid of a pyrrol ring) intermolecular interactions.

(JONKAY; Yang *et al.*, 1991), [Mg(TPP)(H_2O)] (MGPPOR; Timkovich *et al.*, 1969), and [Mg(TTP)(H_2O)] (TTP = 5,10,15,20-tetrakis(4-methylphenyl)porphyrinate) (YONYAF; Meher *et al.*, 2024).

5. Hirshfeld surface analysis

The intermolecular interactions responsible for the crystal cohesion of [Mg(TClPP)$(H_2O)_2$] were also investigated using Hirshfeld surface analysis and two-dimensional fingerprint plots (Turner *et al.*, 2017). The Hirshfeld surfaces were obtained using a standard high surface resolution, mapped over d_{norm} (Fig. 4). As shown in Fig. 4, the red spots correspond to the non-conventional O—H···Cl interactions between the water oxygen atom and the chlorine atoms in the *para*-positions of the four TClPP phenyl rings of neighboring [Mg(TClPP)$(H_2O)_2$] molecules. Similarly, the C7—H7···π interactions (Table 1) are represented as red dots. The d_i *versus* d_e plots shown in Fig. 5 illustrate the distribution of individual intermolecular interactions on the basis of fingerprint maps. The crystal structure is dominated by H···H

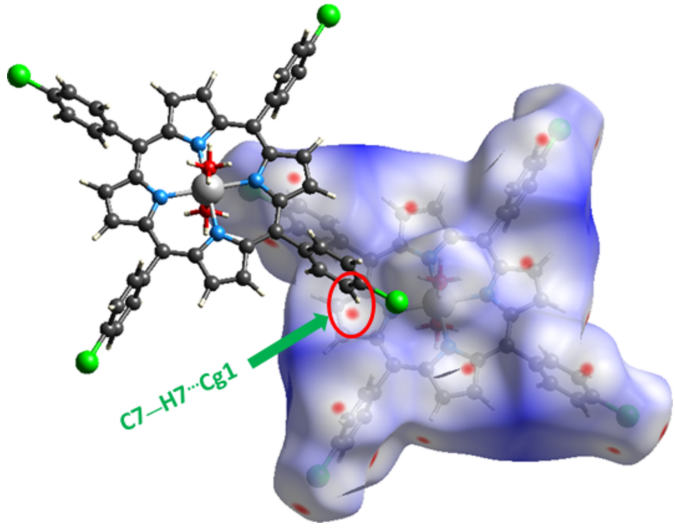

Figure 4
Hirshfeld surface plotted over d_{norm} for the title compound.

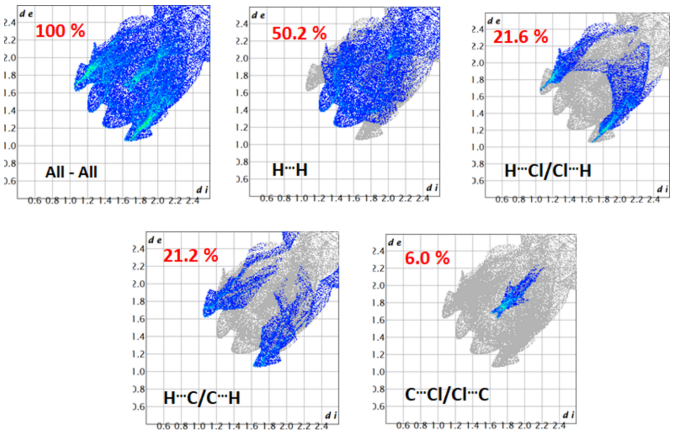

Figure 5
Two-dimensional fingerprint plots showing the distribution of intermolecular interactions responsible for the cohesion of the title complex.

(50.2%) interactions, followed by H···Cl/Cl···H (21.6%), H···C/C···H (21.2%) and C···Cl/Cl···C (6.0) contacts.

6. Synthesis and crystallization of the title complex

In order to prepare the [Mg(TClPP)(ox)] complex (ox = oxalato $C_2O_4^{2-}$), a solution of [Mg(TClPP)] (100 mg, 0.128 mmol) in dichloromethane (40 mL) was added an excess of 18-crown-6 ether (250 mg, 0.946 mmol) and a large excess of $K_2C_2O_4{\cdot}H_2O$ (potassium oxalate monohydrate) (30 mg, 0.163 mol). The reaction mixture was stirred at room temperature for three h and at the end of the reaction, the color of the solution gradually changed from purple to blue. The resulting material was crystallized by diffusion of *n*-hexane through the dichloromethane solution. Single-crystal X-ray diffraction revealed that the crystals obtained correspond to the diaqua–magnesium(II)-TClPP coordination compound. Elemental analysis calculated (%) for $C_{44}H_{28}ClMgN_4O_2$ (M_W = 810.83), C 65.18, H 3.48, N 6.91; found: C 65.49, H 3.61, N 7.12.

7. Refinement

Crystal data, data collection and structure refinement details are given in Table 2. The H-atom position of the axially bonded aqua ligand was found in difference maps and then refined with $U_{iso}(H) = 1.5U_{eq}(O)$. The molecular symmetry of the water molecule is not compatible with the fourfold axis; hence, the occupancy of this H atom was fixed to 0.5. The H atoms attached to C atoms were fixed geometrically and treated as riding with C—H = 0.95 Å and $U_{iso}(H) = 1.5U_{eq}(C)$.

Table 2
Experimental details.

Crystal data	
Chemical formula	$[Mg(C_{44}H_{24}Cl_4N_4)(H_2O)_2]$
M_r	810.81
Crystal system, space group	Tetragonal, *I*4/*m*
Temperature (K)	200
a, *c* (Å)	14.605 (2), 9.4397 (19)
V (Å^3)	2013.5 (7)
Z	2
Radiation type	Mo *Kα*
μ (mm^{-1})	0.35
Crystal size (mm)	0.30 × 0.30 × 0.30
Data collection	
Diffractometer	Bruker AXS Enraf–Nonius Kappa APEXII
Absorption correction	Multi-scan (*SADABS*; Krause *et al.*, 2015)
T_{min}, T_{max}	0.711, 1.000
No. of measured, independent and observed [$I > 2\sigma(I)$] reflections	8146, 1216, 1078
R_{int}	0.032
(sin $\theta/\lambda)_{max}$ (Å^{-1})	0.650
Refinement	
$R[F^2 > 2\sigma(F^2)]$, $wR(F^2)$, *S*	0.041, 0.115, 1.07
No. of reflections	1216
No. of parameters	78
No. of restraints	1
H-atom treatment	H-atom parameters constrained
$\Delta\rho_{max}$, $\Delta\rho_{min}$ (e Å^{-3})	0.32, −0.41

Computer programs: *APEX2* and *SAINT* (Bruker, 2014), *SIR2004* (Burla *et al.*, 2005) and *SHELXL2015* (Sheldrick, 2015).

Acknowledgements

The researcher would like to thank the Deanship of Graduate Studies and Scientific Research at Qassim University for financial support (QU-APC-2026).

References

Amiri, N., Nasri, S., Roisnel, T., Simonneaux, G. & Nasri, H. (2015). *Acta Cryst.* E**71**, m73–m74.
Amiri, N., Dar, U. A., Islam, N., Guergueb, M., Lemercier, G., Chevreux, S. & Nasri, H. (2022). *J. Mol. Struct.* **1248**, 131469.
Barker, A. V. & Pilbeam, D. J. (2015). Editors. *Handbook of Plant Nutrition* 2nd ed. New York: CRC Press.
Borah, B. P., Choudhury, A. K., Majumder, S. J. & Bhuyan, J. (2024). *J. Mol. Struct.* **1306**, 137852.
Borah, K. D. & Bhuyan, J. (2017). *Dalton Trans.* **46**, 6497–6509.
Borah, K. D., Singh, N. G. & Bhuyan, J. (2017). *J. Chem. Sci.* **129**, 449–455.
Bruker (2014). *APEX2* and *SAINT*. Bruker AXS Inc., Madison, Wisconsin, USA.
Burla, M. C., Caliandro, R., Camalli, M., Carrozzini, B., Cascarano, G. L., De Caro, L., Giacovazzo, C., Polidori, G. & Spagna, R. (2005). *J. Appl. Cryst.* **38**, 381–388.
Ezzayani, K., Nasri, S., Belkhiria, M. S., Daran, J.-C. & Nasri, H. (2013). *Acta Cryst.* E**69**, m114–m115.
Fischer, H. & Orth, H. (1937). *Die Chemie des Pyrrols* vol. 2. Leipzig: Akademische Verlag.
Groom, C. R., Bruno, I. J., Lightfoot, M. P. & Ward, S. C. (2016). *Acta Cryst.* B**72**, 171–179.
Gust, D., Moore, T. A. & Moore, A. L. (2001). *Acc. Chem. Res.* **34**, 40–48.
Gutiérrez, A. F., Brittle, S., Richardson, T. H. & Dunbar, A. (2014). *Sens. Actuators B Chem.* **202**, 854–860.
Jabli, S., Hrichi, S., Chaabane-Banaoues, R., Molton, F., Loiseau, F., Roisnel, T., Turowska-Tyrk, I., Babba, H. & Nasri, H. (2022). *J. Mol. Struct.* **1261**, 132882.
Krause, L., Herbst-Irmer, R., Sheldrick, G. M. & Stalke, D. (2015). *J. Appl. Cryst.* **48**, 3–10.
McKee, V. & Rodley, G. A. (1988). *Inorg. Chim. Acta* **151** 233–236.

Meher, S. K., Nayak, P., Dhala, S., Tripathy, S. & Venkatasubbaiah, K. (2024). *Catal. Sci. Technol.* **14**, 3125–3130.
Ong, C. C., McKee, V. & Rodley, G. A. (1986). *Inorg. Chim. Acta* **123**, L11–L14.
Sheldrick, G. M. (2015). *Acta Cryst.* C**71**, 3–8.
Singh, N. G., Borah, K. D. & Bhuyan, J. (2022). *Inorg. Chim. Acta* **542**, 121145.
Timkovich, R. & Tulinsky, A. (1969). *J. Am. Chem. Soc.* **91**, 4430–4432.
Turner, M. J., McKinnon, J. J., Wolff, S. K., Grimwood, D. J., Spackman, P. R., Jayatilaka, D. & Spackman, M. A. (2017). *CrystalExplorer17*. University of Western Australia.
Woodward, R. B., Ayer, W. A., Beaton, J. M., Bickelhaupt, F., Bonnett, R., Buchschacher, P., Closs, G. L., Dutler, H., Hannah, J., Hauck, F. P., Itô, S., Langemann, A., Le Goff, E., Leimgruber, W., Lwowski, W., Sauer, J., Valenta, Z. & Volz, H. (1960). *J. Am. Chem. Soc.* **82**, 3800–3802.
Yang, S. & Jacobson, R. A. (1991). *Inorg. Chim. Acta* **190**, 129–134.

supporting information

Acta Cryst. (2026). E**82**, 249-253 [https://doi.org/10.1107/S2056989026000836]

Crystal structure and Hirshfeld surface analysis of the coordination compound diaqua[5,10,15,20-tetrakis(4-chlorophenyl)porphyrinato-κ^4N]magnesium(II)

Mona A. Alamri

Computing details

Diaqua[5,10,15,20-tetrakis(4-chlorophenyl)porphyrinato-κ^4N]magnesium(II)

Crystal data

$[Mg(C_{44}H_{24}Cl_4N_4)(H_2O)_2]$
M_r = 810.81
Tetragonal, *I*4/*m*
a = 14.605 (2) Å
c = 9.4397 (19) Å
V = 2013.5 (7) Å^3
Z = 2
F(000) = 832
D_x = 1.337 Mg m^{-3}
Mo *Kα* radiation, λ = 0.71073 Å
Cell parameters from 8167 reflections
θ = 2.6–27.5°
μ = 0.35 mm^{-1}
T = 200 K
Block, blue
0.30 × 0.30 × 0.30 mm

Data collection

Bruker AXS Enraf–Nonius Kappa APEXII diffractometer
Radiation source: Incoatec ISG250
φ and ω scans
Absorption correction: multi-scan (SADABS; Krause *et al.*, 2015)
T_{min} = 0.711, T_{max} = 1
8146 measured reflections
1216 independent reflections
1078 reflections with $I > 2\sigma(I)$
R_{int} = 0.032
θ_{max} = 27.5°, θ_{min} = 2.6°
h = −18→18
k = −17→18
l = −9→12

Refinement

Refinement on F^2
Least-squares matrix: full
$R[F^2 > 2\sigma(F^2)]$ = 0.041
$wR(F^2)$ = 0.115
S = 1.07
1216 reflections
78 parameters
1 restraint
Hydrogen site location: mixed
H-atom parameters constrained
$w = 1/[\sigma^2(F_o^2) + (0.056P)^2 + 1.969P]$ where $P = (F_o^2 + 2F_c^2)/3$
$(\Delta/\sigma)_{max} < 0.001$
$\Delta\rho_{max}$ = 0.32 e Å^{-3}
$\Delta\rho_{min}$ = −0.41 e Å^{-3}

Special details

Geometry. All esds (except the esd in the dihedral angle between two l.s. planes) are estimated using the full covariance matrix. The cell esds are taken into account individually in the estimation of esds in distances, angles and torsion angles; correlations between esds in cell parameters are only used when they are defined by crystal symmetry. An approximate (isotropic) treatment of cell esds is used for estimating esds involving l.s. planes.

Fractional atomic coordinates and isotropic or equivalent isotropic displacement parameters (Å²)

	x	*y*	*z*	U_{iso}*/U_{eq}	Occ. (<1)
Mg1	0.5000	−0.5000	0.0000	0.0360 (4)	
N1	0.53951 (11)	−0.36427 (11)	0.0000	0.0283 (4)	
C4	0.33650 (13)	−0.20277 (14)	0.0000	0.0290 (4)	
C1	0.48278 (14)	−0.28960 (13)	0.0000	0.0278 (4)	
C5	0.33189 (14)	−0.37233 (14)	0.0000	0.0286 (4)	
C3	0.38633 (13)	−0.29286 (13)	0.0000	0.0275 (4)	
C8	0.24114 (15)	−0.03956 (14)	0.0000	0.0370 (5)	
C6	0.31214 (13)	−0.16133 (12)	0.1253 (2)	0.0463 (5)	
H6	0.3285	−0.1893	0.2126	0.056*	
O1	0.5000	−0.5000	0.2381 (3)	0.0583 (7)	
H10	0.5516	−0.5286	0.2938	0.070*	0.5
C7	0.26386 (14)	−0.07894 (12)	0.1262 (2)	0.0503 (5)	
H7	0.2471	−0.0508	0.2131	0.060*	
Cl1	0.17689 (4)	0.06145 (4)	0.0000	0.0588 (3)	
C2	0.53683 (15)	−0.20673 (14)	0.0000	0.0320 (5)	
H2	0.5142	−0.1457	0.0000	0.038*	
C9	0.23260 (14)	−0.37383 (14)	0.0000	0.0311 (4)	
H9	0.1931	−0.3221	0.0000	0.037*	

Atomic displacement parameters (Å²)

	U^{11}	U^{22}	U^{33}	U^{12}	U^{13}	U^{23}
Mg1	0.0233 (4)	0.0233 (4)	0.0615 (10)	0.000	0.000	0.000
N1	0.0240 (8)	0.0228 (8)	0.0381 (10)	−0.0006 (6)	0.000	0.000
C4	0.0270 (9)	0.0245 (9)	0.0354 (11)	0.0016 (7)	0.000	0.000
C1	0.0295 (10)	0.0232 (9)	0.0307 (10)	0.0003 (7)	0.000	0.000
C5	0.0262 (9)	0.0271 (9)	0.0326 (10)	0.0032 (7)	0.000	0.000
C3	0.0277 (9)	0.0246 (9)	0.0303 (10)	0.0036 (7)	0.000	0.000
C8	0.0268 (10)	0.0232 (9)	0.0609 (15)	0.0026 (8)	0.000	0.000
C6	0.0605 (11)	0.0423 (9)	0.0361 (9)	0.0202 (8)	−0.0061 (8)	−0.0041 (7)
O1	0.0619 (10)	0.0619 (10)	0.0510 (16)	0.000	0.000	0.000
C7	0.0599 (11)	0.0429 (9)	0.0481 (11)	0.0190 (8)	−0.0033 (9)	−0.0148 (8)
Cl1	0.0414 (4)	0.0271 (3)	0.1078 (7)	0.0095 (2)	0.000	0.000
C2	0.0349 (10)	0.0218 (9)	0.0393 (11)	−0.0021 (8)	0.000	0.000
C9	0.0246 (9)	0.0310 (10)	0.0377 (11)	0.0050 (8)	0.000	0.000

Geometric parameters (Å, º)

Mg1—N1^{i}	2.0646 (17)	C5—C3	1.407 (3)
Mg1—N1^{ii}	2.0646 (17)	C5—C9	1.450 (3)
Mg1—N1^{iii}	2.0646 (17)	C8—C7	1.364 (2)
Mg1—N1	2.0646 (17)	C8—C7^{iv}	1.364 (2)
Mg1—O1^{i}	2.248 (3)	C8—Cl1	1.748 (2)
Mg1—O1	2.248 (3)	C6—C7	1.395 (2)
N1—C1	1.370 (3)	C6—H6	0.9500

N1—C5^{ii}	1.372 (3)	O1—H10	1.0100
C4—C6^{iv}	1.376 (2)	C7—H7	0.9500
C4—C6	1.376 (2)	C2—C9^{ii}	1.358 (3)
C4—C3	1.504 (3)	C2—H2	0.9500
C1—C3	1.409 (3)	C9—C2^{iii}	1.358 (3)
C1—C2	1.445 (3)	C9—H9	0.9500
C5—N1^{iii}	1.372 (3)		

N1^{i}—Mg1—N1^{ii}	90.0	C3—C1—C2	125.05 (19)
N1^{i}—Mg1—N1^{iii}	90.0	N1^{iii}—C5—C3	125.41 (18)
N1^{ii}—Mg1—N1^{iii}	180.00 (9)	N1^{iii}—C5—C9	109.30 (17)
N1^{i}—Mg1—N1	180.0	C3—C5—C9	125.28 (18)
N1^{ii}—Mg1—N1	89.999 (1)	C5—C3—C1	126.35 (18)
N1^{iii}—Mg1—N1	90.001 (1)	C5—C3—C4	116.63 (17)
N1^{i}—Mg1—O1^{i}	90.0	C1—C3—C4	117.01 (17)
N1^{ii}—Mg1—O1^{i}	90.0	C7—C8—C7^{iv}	121.7 (2)
N1^{iii}—Mg1—O1^{i}	90.0	C7—C8—Cl1	119.11 (10)
N1—Mg1—O1^{i}	90.0	C7^{iv}—C8—Cl1	119.11 (10)
N1^{i}—Mg1—O1	90.0	C4—C6—C7	121.01 (17)
N1^{ii}—Mg1—O1	90.0	C4—C6—H6	119.5
N1^{iii}—Mg1—O1	90.0	C7—C6—H6	119.5
N1—Mg1—O1	90.0	Mg1—O1—H10	121.4
O1^{i}—Mg1—O1	180.0	C8—C7—C6	118.81 (17)
C1—N1—C5^{ii}	107.05 (16)	C8—C7—H7	120.6
C1—N1—Mg1	126.55 (13)	C6—C7—H7	120.6
C5^{ii}—N1—Mg1	126.40 (14)	C9^{ii}—C2—C1	106.96 (18)
C6^{iv}—C4—C6	118.6 (2)	C9^{ii}—C2—H2	126.5
C6^{iv}—C4—C3	120.67 (10)	C1—C2—H2	126.5
C6—C4—C3	120.67 (10)	C2^{iii}—C9—C5	107.02 (18)
N1—C1—C3	125.28 (18)	C2^{iii}—C9—H9	126.5
N1—C1—C2	109.67 (18)	C5—C9—H9	126.5

Symmetry codes: (i) −*x*+1, −*y*−1, −*z*; (ii) *y*+1, −*x*, −*z*; (iii) −*y*, *x*−1, *z*; (iv) *x*, *y*, −*z*.

Hydrogen-bond geometry (Å, º)

*Cg*1 and *Cg*2 are the centroids of the N1,C1,C2,C9″,C5″ and C5,C9,C2′,C1′,N1′ rings, respectively. Symmetry codes: (′) -*y*, -1 + *x*, *z*; (″) 1 + *y*, -*x*, *z*.

D—H···*A*	*D*—H	H···*A*	*D*···*A*	*D*—H···*A*
C7—H7···*Cg*1^{v}	0.95	2.75	3.608 (2)	150
C7—H7···*Cg*2^{vi}	0.95	2.75	3.608 (2)	150
O1—H10···Cl1^{vii}	1.01	2.92	3.691 (2)	128

Symmetry codes: (v) *y*+1/2, −*x*+1/2, *z*+1/2; (vi) −*x*+1/2, −*y*−1/2, *z*+1/2; (vii) *x*+1/2, *y*−1/2, *z*+1/2.